TURBULENT HEAT TRANSFER IN CHANNEL FLOW WITH NON-ORTHOGONAL SYSTEM ROTATION

Haibin Wu
Department of Mechanical Engineering
The University of Tokyo
Hongo 7-3-1, Bunkyo ku, Tokyo 113-8656, Japan
wu@thtlab.t.u-tokyo.ac.jp

Nobuhide Kasagi
Department of Mechanical Engineering
The University of Tokyo
Hongo 7-3-1, Bunkyo ku, Tokyo 113-8656, Japan
kasagi@thtlab.t.u-tokyo.ac.jp

Keywords: turbulent heat transfer, non-orthogonal system rotation, direct numerical simulation

ABSTRACT

Direct numerical simulations of a fully developed turbulent channel flow with combined system rotations have been performed. A pseudo-spectral method is used to solve the unsteady Navier-Stokes equation and the heat convection equation in a reference frame rotating with the system. The Reynolds number, based on the x-direction bulk mean velocity and the half-width of the channel, and the Prandtl number are set to 4560 and 0.71, respectively.

In a channel with combined spanwise and streamwise system rotations, two cases are considered. In the first case, the absolute rotation number is kept constant for three values, 5, 7.5 and 11, and the angle between the rotating axis and the positive x-direction is increased from 0 to 90° (case I). In the other case, the spanwise rotation number is set to 2.5 and the streamwise rotation number is increased to 15 (case II). Also considered in a channel with combined wall-normal and spanwise rotations are two cases: a constant wall-normal rotation number 0.04 with the spanwise rotation number increased to 15 (case III) and a constant spanwise rotation number 2.5 with the wall-normal rotation number increased to 0.04 (case IV).

The results of the present simulation for a spanwise rotating channel and for a streamwise rotating channel are compared with those by Kristoffersen *et al.* (1993) and by Elsamni (2001), respectively. Good agreements between these results validate the present simulations.

As the angle is increased in case I, the Nusselt number has a similar tendency to that in the single spanwise rotating channel with increasing the spanwise rotation number. On the suction side, however, the Nusselt number has some local maxima at 45° for all the three absolute rotation numbers considered presently. The ratio of the heat flux on the wall to the total friction also reaches a local maximum at this angle. The similar tendencies of the mean properties and the temperature statistics to those in the single spanwise rotating channel reveal the dominant effect of the spanwise rotation.

In case II, the increment of the streamwise rotation number enhances the heat transfer on both walls, especially for the streamwise rotation numbers larger than the twice spanwise rotation number. This tendency is different from that in the flow field, where the turbulence is mainly enhanced along the suction side.

The changes of most statistics in case III are quite similar to those in the single spanwise rotating channel. The Nusselt number, however, is comparatively larger than that in the single spanwise rotating channel, especially for the spanwise rotation number larger than 7.5 on the pressure side.

If the spanwise rotation number is kept constant and just the wall-normal rotation number is increased (case IV), an increasingly larger and asymmetric spanwise mean velocity is induced. The changes of the streamwise mean velocity and the mean temperature are comparatively small. The wall-normal rotation enhances the Nusselt number mainly along the suction side.

The visualization of the temperature fluctuation in x-z planes reveals the existence of streaks between high and low temperatures in the near wall region, similar to the streaky structures of the streamwise velocity fluctuation. The spanwise rotation increases the number and intensity of these streaks on the pressure side, but reduces on the suction side. In case II, the increasing of the streamwise rotation number enhances these streaky structures on both walls, but more evidently on the suction side. These structures drift towards positive or negative z direction, coinciding with the sign of the spanwise mean velocity on the two walls. In case IV, these streaky structures are only enhanced slightly, but the tilting direction is changed to the positive z direction.

Roman symbols

C_f	friction coefficient, $C_f = 2\tau_w / \rho U_m^2$
F	total friction across the channel $F = \tau_{wp} + \tau_{ws}$
Nu	Nusselt number, $Nu = -2\delta Q_w / (T_m - T_w)\lambda$
Pr	Prandtl number
Q_w	heat flux on the wall, $Q_w = -\lambda(dT/dy)_w$
Re_b	Reynolds number, $Re_b = 2U_m\delta/\upsilon$
Re_τ	Reynolds number, $Re_\tau = u_\tau\delta/\upsilon$
Ro	absolute rotation number, $Ro = 2\delta\Omega/u_\tau$
Ro_i	rotation number in i-th direction $Ro_i = 2\delta\Omega_i/u_\tau$
U, W	streamwise and spanwise mean velocities
x, y, z	streamwise, wall-normal and spanwise directions
T	mean temperature
T_{lower}	the temperature on the lower wall
T_{upper}	the temperature on the upper wall
ΔT	the temperature difference between two walls
t'	temperature fluctuation
u_i	velocity component in i-th direction
u_τ	friction velocity

Greek symbols

τ	shear stress
Ω	angular velocity of system rotation
δ	channel half-width
λ	thermal conductivity
β	the angle between the absolute between the rotating axis and x- direction
θ	temperature
υ	kinematic viscosity

Subscript and superscript

m	bulk averaged
w	value on the wall
p	value on the pressure side
s	value on the suction side
i	i-th direction
o	value in the non-rotating channel

INTRODUCTION

For the past several decades, a lot of experiments and numerical simulations have been performed to investigate the essence of rotating turbulent flows, since these flows exist widely in industrial, geophysical and astrophysical applications. The Coriolis force arisen from the system rotation influences both the mean flow and the turbulence, so that the momentum and heat transfers in rotating turbulent flows should be different from those in non-rotating cases.

The experiment of a spanwise rotating channel by Johnston *et al.* [1] revealed that the turbulence was enhanced near the pressure side of the channel, but reduced along the suction side. This phenomenon was confirmed by Kim [2] in his large eddy simulation (hereafter LES) for a spanwise rotating channel with a Reynolds number equal to 13,800, based on the centerline velocity and the half-width of the channel. Kristoffersen and Andersson [3] performed their direct numerical simulations (hereafter DNS) for a spanwise rotating channel, in which the rotation number, based on the bulk mean velocity and the channel half-width, varied from 0 to 0.5. They found that the augmentation and damping of the turbulence along the pressure side and the suction side, respectively, became more significant with increasing the rotation number. Rotational-induced roll cells nearer to the pressure side were also identified. Besides the spanwise rotating channels, Oberlack [5] applied the lie group analysis of the two-point correlation equations, LES and DNS for a streamwise rotating channel and found that both of the streamwise and the induced spanwise mean velocities had some linear scaling laws and all six components of the Reynolds stresses tensor were non-zero.

Recently, a series of studies about the momentum and heat transfers in orthogonal rotating channels, in which the rotating axis was parallel to one of the three coordinate axes, were carried about by Elsamni [6]. In his DNS, the Reynolds number was set to 150 and the rotation number was increased from 0 to 15 for the spanwise and streamwise rotating channels and from 0 to 0.04 for a wall-normal rotating channel (both Reynolds number and rotation number based on the friction velocity and the channel half-width). For the spanwise rotating channel, it was found that both of the Nusselt number and friction coefficient first increased with the rotation number, but decreased after some critical rotation numbers on the pressure side. On the suction side, these two terms decreased monotonously with increasing the rotation number. In the streamwise rotating channel, an induced spanwise mean velocity was skew-symmetric with respective to the center of the channel and the absolute values of the peaks increased with the rotation number. The Nusselt number and friction coefficient became increasingly larger as the rotation number was increased. Although the rotation number in the wall-normal rotating channel was two-order smaller than those in the spanwise and streamwise rotating channels, a quite large spanwise mean velocity was induced. The increased Nusselt number and friction coefficient were observed with increasing the rotation number in this case.

In real applications, however, the rotating axis is not always parallel to some certain coordinate axis, so that the Coriolis forces arisen from different rotating directions should interact with each other, which results in more complex momentum and heat transfers. The present study aims to probe the combined effects of different Coriolis forces in heat transfer. Considered presently are two cases, in which the rotating axis is parallel to the x-z and y-z planes, respectively.
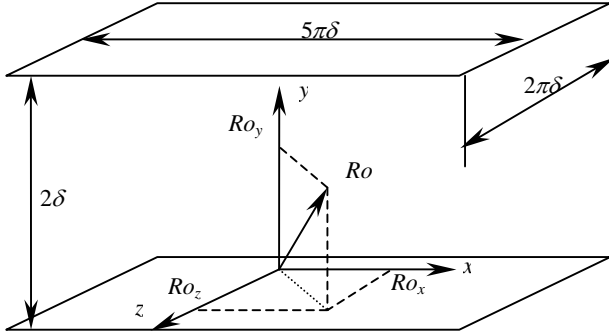
Fig. 1 Channel flow with non-orthogonal system rotation.

NUMERICAL METHOD AND VALIDATION
Numerical method

In the present study, we consider a rotating turbulent flow in a plane channel as shown in Fig. 1. Homogeneity is assumed in the streamwise x and the spanwise z directions with a computation domain of $5\pi\delta \times 2\delta \times 2\pi\delta$ in x, y and z directions, respectively. The bulk mean velocity in x direction is kept constant 15.2 with adjusting the mean pressure gradient in this direction and the temperatures on the two walls are kept constant with a higher one on the lower wall. The governing equations for this problem with neglecting the buoyancy can be written as follows:

$$\frac{\partial u_i}{\partial t} = -\frac{\partial P}{\partial x_i} + \frac{1}{\mathrm{Re}_\tau}\frac{\partial^2 u_i}{\partial x_j^2} - u_j \frac{\partial u_i}{\partial x_j} - \varepsilon_{ijk} Ro_j u_k , \qquad (1)$$

$$\frac{\partial \theta}{\partial t} = \frac{1}{\mathrm{Re}_\tau \mathrm{Pr}}\frac{\partial^2 \theta}{\partial x_j \partial x_j} - u_j \frac{\partial \theta}{\partial x_j} , \qquad (2)$$

$$\frac{\partial u_i}{\partial x_i} = 0 . \qquad (3)$$

All the variables in these equations are normalized by the friction velocity in the non-rotating channel $u_{\tau o}$, the half-width of the channel δ and the temperature difference on the two walls ΔT.

In order to solve the governing equations, a pseudo-spectral method is employed with Fourier series expansions in homogeneous directions and Chebyshev polynomials in the wall-normal direction for the spatial discretization. The Crank-Nicolson and Adams-Bashforth schemes are used for the viscous terms and nonlinear terms, respectively, in time integration. A $64 \times 65 \times 64$ grid system with constant grid widths in homogenous directions and non-uniform in the wall-normal direction is applied to the present DNS. The time integration is extended to $12\delta/u_\tau$ for sampling statistics with a time step $0.12\delta^2/\upsilon$ after the flow reaches a fully developed state, in which the total stress across the channel becomes linear.

Validation of the present DNS

DNS is a powerful tool in the study of flow dynamics. In order to validate the present DNS, the results for a spanwise rotating channel and a streamwise rotating channel are compared with the former accurate DNS by Kristoffersen et al. [3] and by Elsamni [4], respectively, as shown in Fig. 2.

The streamwise mean velocities in the present DNS and in that by Kristoffersen et al. for a spanwise rotating channel are compared in Fig. 2 (a). Although there is a small difference between the two rotation numbers, the agreement is still quite good. The comparison of the spanwise mean velocity for a streamwise rotating channel is plotted in Fig. 2 (b). The present result with a coarse grid system has higher absolute peaks near the central part of the channel, but slightly smaller ones near the two walls.
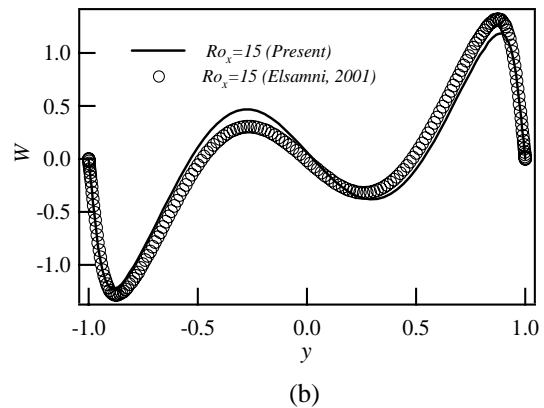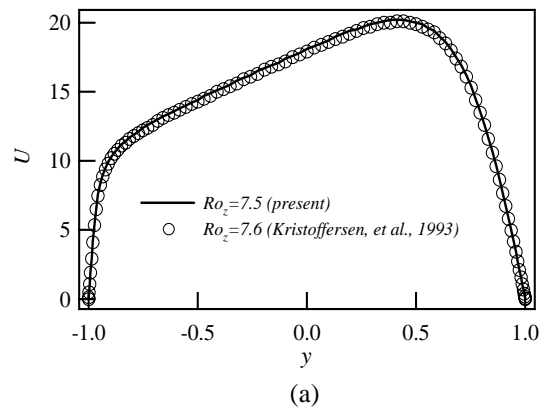

(a)

(b)

Fig. 2 Validation of present DNS in the spanwise and streamwise rotating channels (a) the streamwise mean velocity in a spanwise rotating channel; (b) the spanwise mean velocity in a streamwise rotating channel.

RESULTS AND DISCUSSION
Combined streamwise and spanwise rotations

For combined streamwise and spanwise rotations in a turbulent channel, two cases are considered presently. In case I, the absolute rotation number is kept constant for three values, 5, 7.5 and 11, and the angle β between the rotating axis and the positive x-direction is changed to five different values, 0, 30, 45, 60 and 90° (see Fig. 3 (a)). In case II, the spanwise rotation number Ro_z is set to 2.5 and only the streamwise rotation number Ro_x is increased to 15 as shown in Fig. 3 (b).
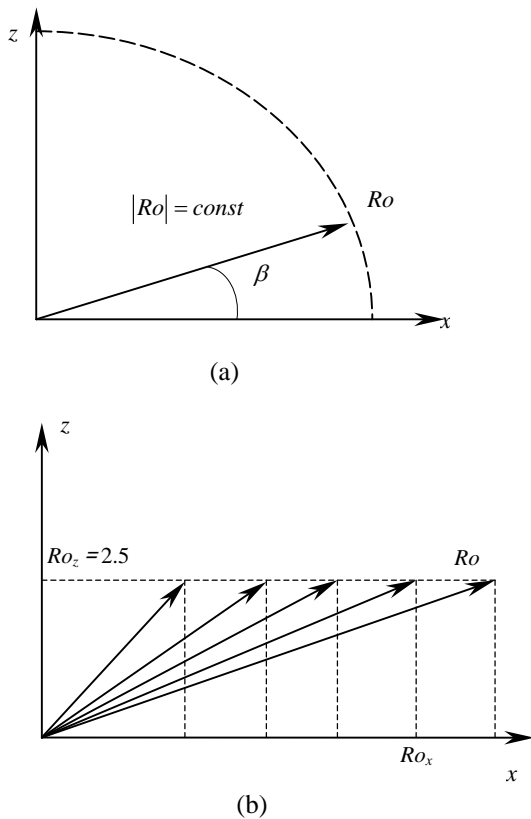
Fig. 3 Rotation vector of combined streamwise and spanwise system rotations (a) Case I; (b) Case II.

Case I

The Nusselt number in case I normalized by that in a non-rotating channel is plotted in Fig. 4. For the absolute rotation numbers, 7.5 and 11, the maximum values on the pressure side appear at the angle of 45 and 30°. For $Ro = 5$, however, the maximum value arises at 90°. The local maximum values of Nu come forth at 45° on the suction side. Except some local maxima on the suction side, the general trend of Nu is similar to that in the single spanwise rotating channel, which reveals the dominant effect of the spanwise rotation. The ratio of the heat flux on the wall Q_w to the total friction F reaches a local maximum at 45° as shown in Fig. 5.

The streamwise and spanwise mean velocities and the mean temperature in case I are shown in Fig. 6. Here, only the results for $Ro = 7.5$ are given and those for the other absolute rotation numbers have similar tendencies. The slope of the linear regime in the streamwise mean velocity becomes increasingly larger and the gradient of the mean temperature on the two walls decreases with increasing β. The change of the spanwise mean velocity is quite complicated, but we can see that at 45° this term reaches a minimum at the central part of the channel and a second largest peak near the suction side.

The root mean square (hereafter rms) value of the temperature fluctuation and the turbulent heat fluxes are drawn in Fig. 7. The term t'_{rms} decreases with increasing

β, which is similar to that in the single spanwise rotating channel. The two components of the turbulent heat fluxes $\overline{ut}$ and $\overline{vt}$ are suppressed by increasing β, but recover to some extent at 45°. The other term $\overline{wt}$ on the suction side fist increases with β, reaches maximum at 45° and then begins to decrease again. On the pressure side, however, this term decreases continuously with increasing β.

Case I shows some similar tendencies to those in the single spanwise rotating channel, but some different trends can be also detected, especially some local maxima or peaks at the angle of 45°. These statistics reveal that the spanwise rotating effect is dominant in case I, but the streamwise rotating effect is also appreciable mainly on the suction side.
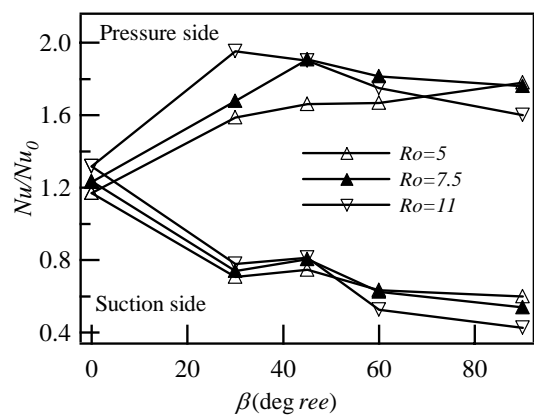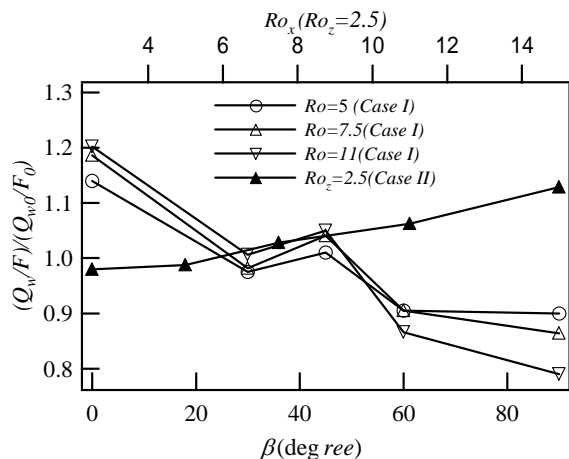

Fig. 4 Nusselt number in case I.

Fig. 5 Ratio of the heat flux on the wall to the total friction in Case I and II.

Case II

The Nusselt number in case II is shown in Fig. 8. This term increases quite obviously for Ro_x larger than 5, two times of the spanwise rotation number Ro_z. The Nusselt number in the single streamwise rotating channel is also given in this figure. The ratio of heat flux on the wall Q_w to the total friction F increases with Ro_x as shown in Fig. 5.
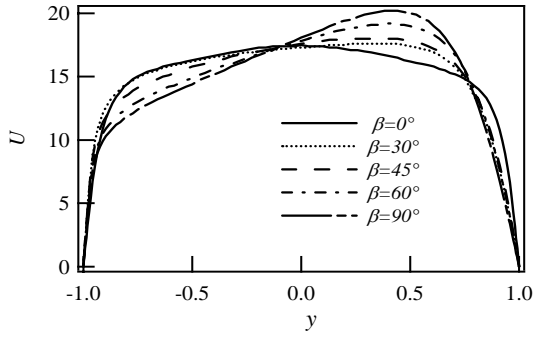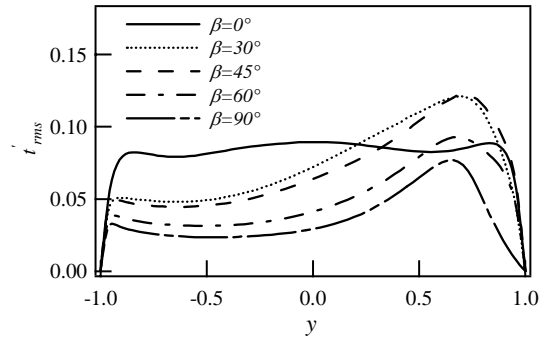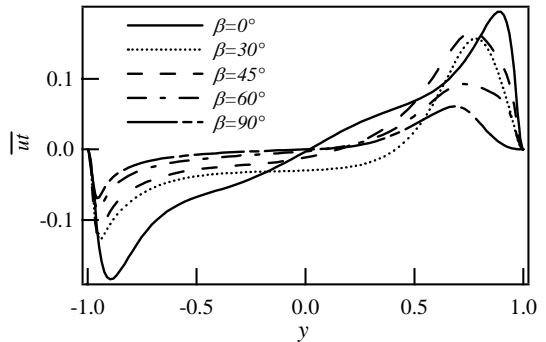
(a)
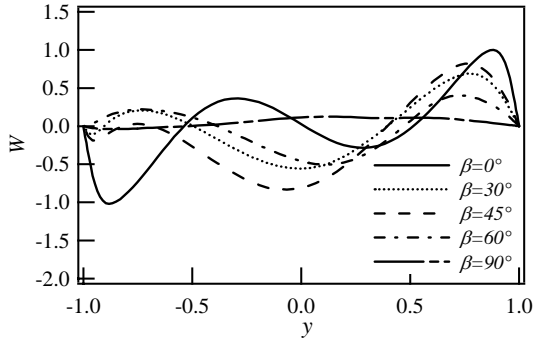
(b)
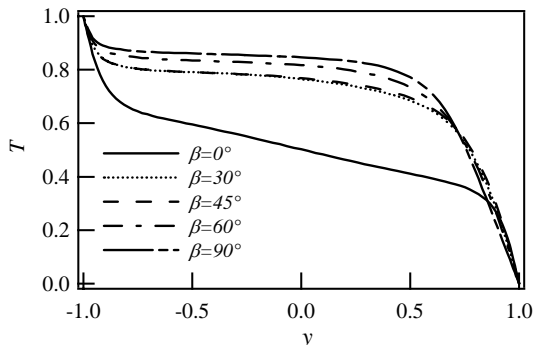
(c)

Fig. 6 The mean properties in case I (a) the streamwise mean velocity; (b) the spanwise mean velocity; (c) the mean temperature.

Figure 9 denotes the mean properties in case II. The gradient of the streamwise mean velocity increases with Ro_x on the suction side, but near the pressure side this term only changes slightly. The spanwise mean velocity has drastic enhancement on the suction side for Ro_x larger than 5, while decreases on the pressure side. Comparing the changes of W on the two sides, we can see that the enhancement on the suction side is much more remarkable. The gradients of the mean temperature on the both walls increase with Ro_x, the bulk mean temperature decreases and the asymmetry of the profile is gradually reduced.
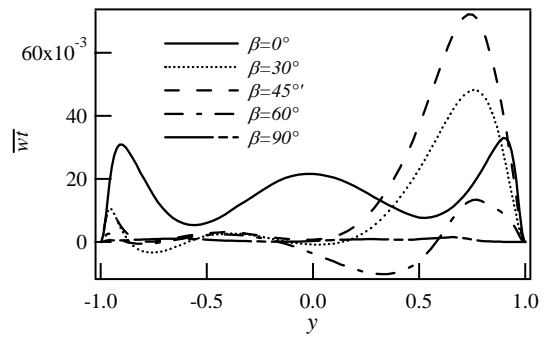

(a)

(b)
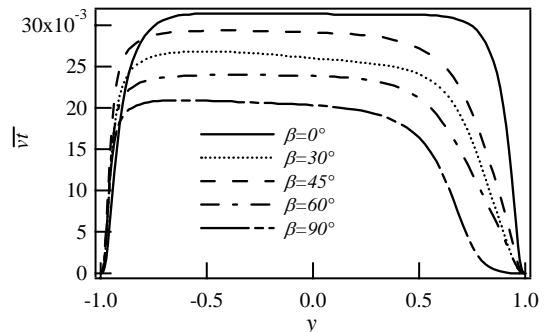
(c)

(d)

Fig. 7 Statistics in case I (a) Rms temperature fluctuation; heat fluxes (b) $\overline{ut}$; (c) $\overline{vt}$; (d) $\overline{wt}$.
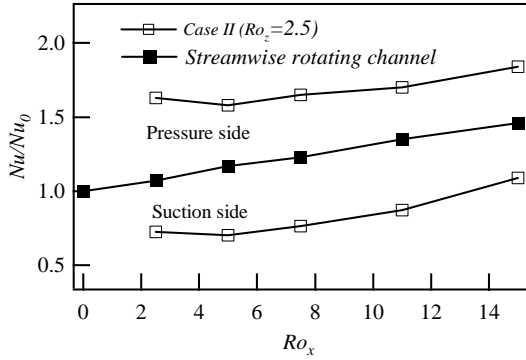
Fig. 8 Nusselt number in case II and a single streamwise rotating channel.
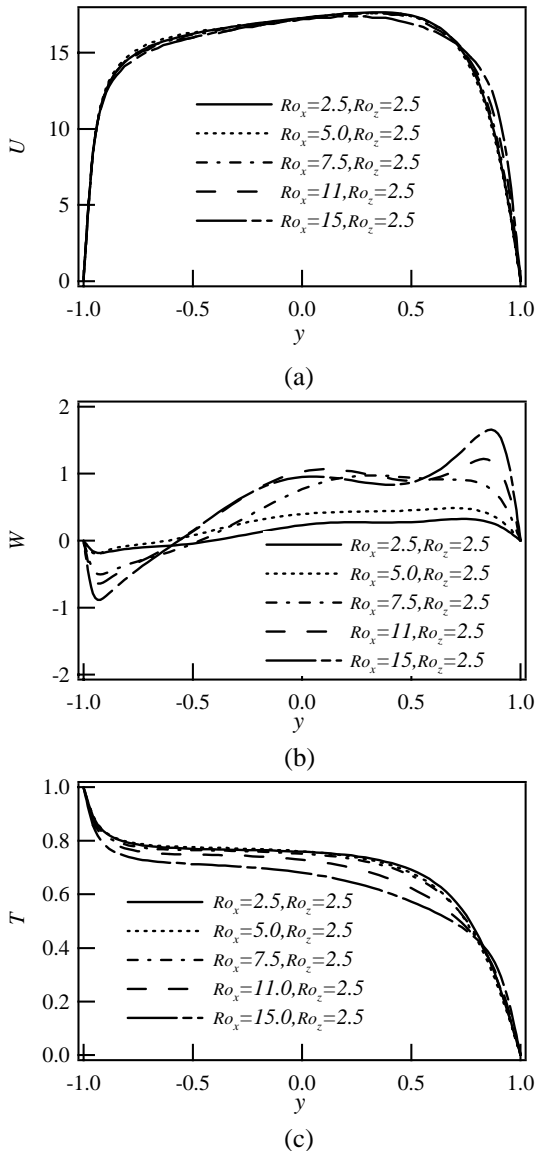

(a)

(b)

(c)

Fig. 9 Mean properties in case II (a) the streamwise mean velocity; (b) the spanwise mean velocity; (c) the mean temperature.
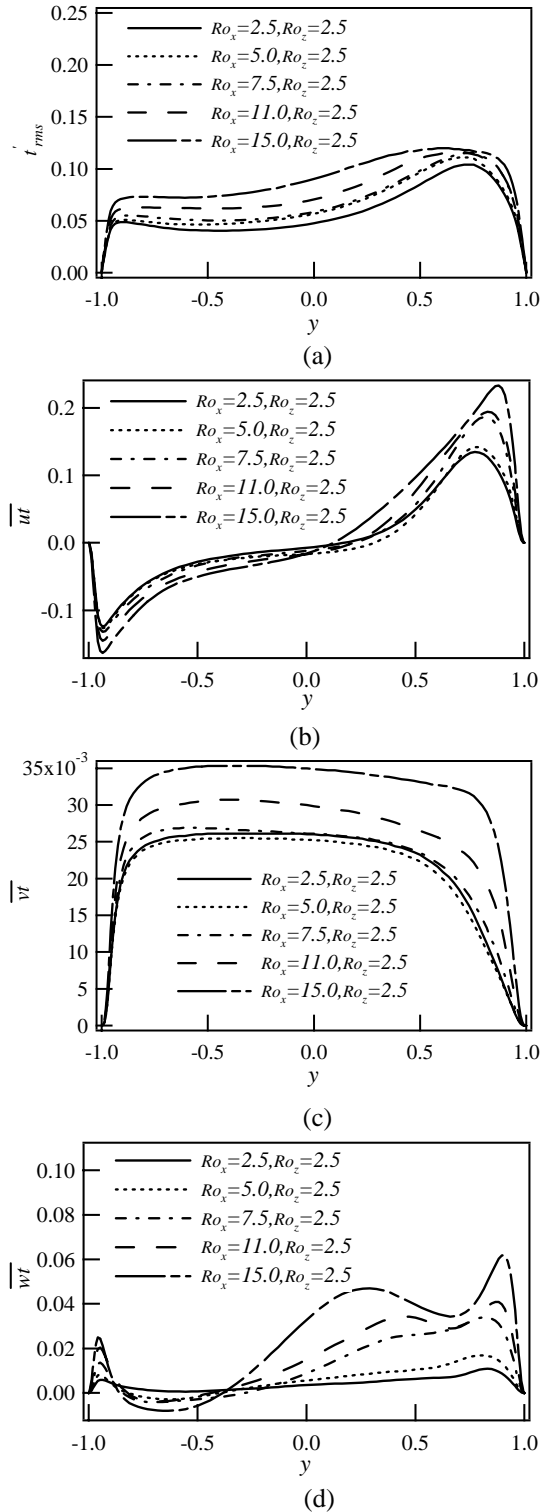

(a)

(b)

(c)

(d)

Fig. 10 Statistics in case II (a) Rms temperature fluctuation; heat fluxes (b) $\overline{ut}$; (c) $\overline{vt}$; (d) $\overline{wt}$.

For the flow field, the increasing of the streamwise rotation number enhances the turbulence mainly along the suction side (not shown here). For the temperature field, however, the rms temperature fluctuation and the turbulent heat fluxes are all enhanced obviously on both walls as shown in Fig. 10. This difference comes from the

6

following facts. In the flow field, the energy transfer from the mean flow to the turbulence is tightly concerned with the term dU/dy, which increases obviously near the suction side but slightly on the pressure side with increasing Ro_x. On the contrary, in the temperature field, the production terms of t'_{rms} and the turbulent heat fluxes are all influenced by the term dT/dy, which is equally enhanced on both walls.
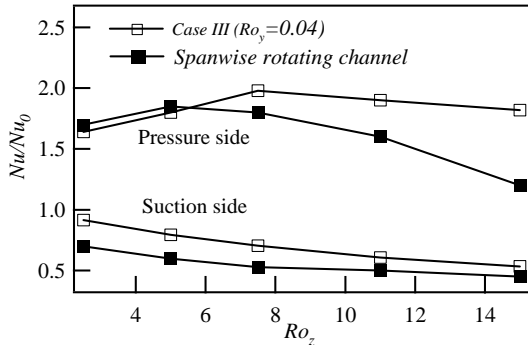
Fig.11 Nusselt number in case III and a single spanwise rotating channel.

Combined wall-normal and spanwise rotations

Elsamni [6] performed DNS for a wall-normal rotating channel. Although the rotation number Ro_y was two orders smaller than those in the spanwise and streamwise rotating channels, a quite large spanwise mean velocity was induced. In the present study, the combined effects of wall-normal and spanwise rotations are probed. In one case, the wall-normal rotation number Ro_y is set to 0.04 and the spanwise rotation number Ro_z is increased to 15 (case III), while, in the other case, Ro_z is set to 2.5 and Ro_y is increased to 0.04 (case IV).

Case III

The change of the Nusselt number in case III resembles that in the single spanwise rotating channel. The wall-normal rotation, however, increases Nu on both sides, especially for Ro_z larger than 7.5 on the pressure side as shown in Fig. 11.

The mean properties in case III are plotted in Fig. 12. Both U and W have linear regimes and the slopes increase with Ro_z. The gradient of the mean temperature on both walls decreases and the bulk mean temperature increases with increasing Ro_z.

The rms temperature fluctuation t'_{rms} and the two components of the heat fluxes $\overline{ut}$ and $\overline{vt}$ decrease with increasing Ro_z, which is the same as that in the single spanwise rotating channel. The wall-normal rotation induces a new component of the heat fluxes $\overline{wt}$ as shown in Fig. 13. Higher spanwise rotation number Ro_z reduces $\overline{wt}$ on both walls, but the reduction on the pressure side is comparatively larger than that on the suction side.
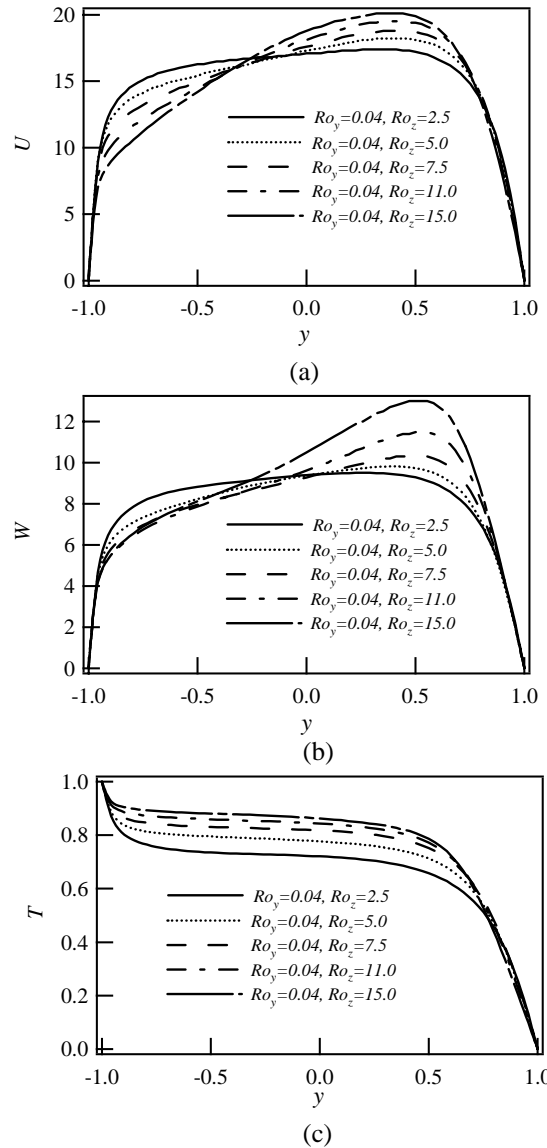
Fig. 12 Mean properties in case III (a) the streamwise mean velocity; (b) the spanwise mean velocity; (c) the mean temperature.
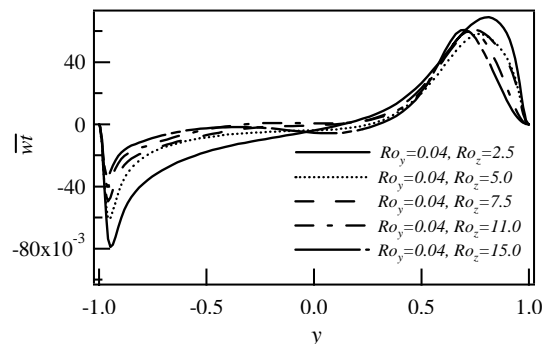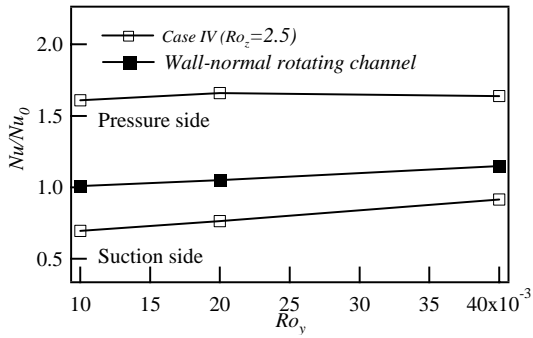
Fig. 13 Heat flux $\overline{wt}$ in case III.

Fig. 14 Nusselt number in case IV and a single wall-normal rotating channel.

however, this term keeps almost constant (see Fig. 14). These facts express that the wall-normal rotation mainly enhances the heat transfer along the suction side, but on the pressure side the spanwise rotation is still the dominant factor.
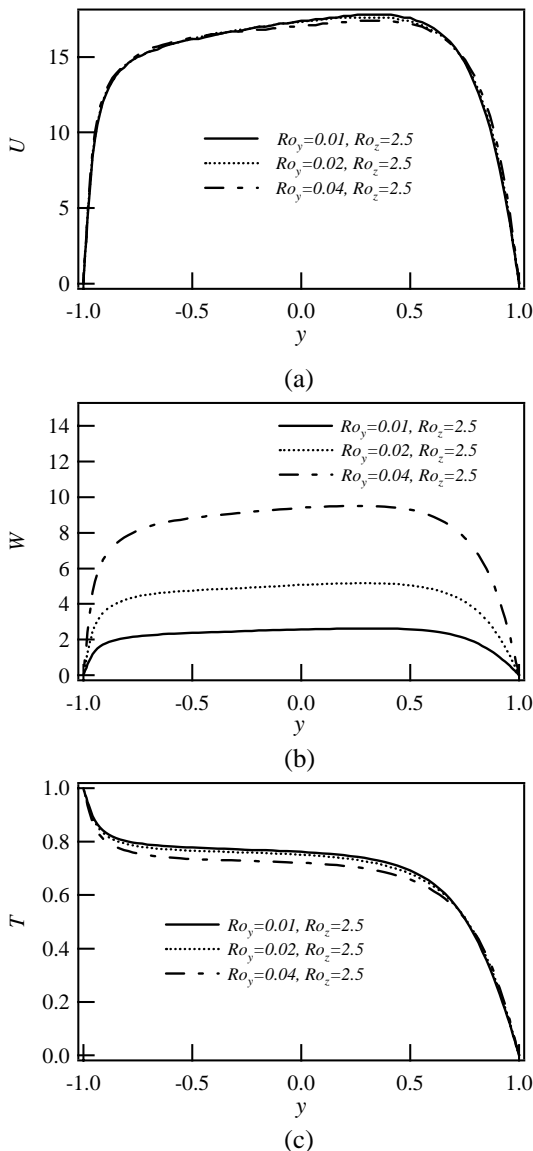

(a)

(b)

(c)

Fig. 15 Mean properties in case IV (a) the streamwise mean velocity; (b) the spanwise mean velocity; (c) the mean temperature.

Case IV

The Nusselt number on the suction side in case IV increases at the similar pace to that in the single wall-normal rotating channel. On the pressure side,
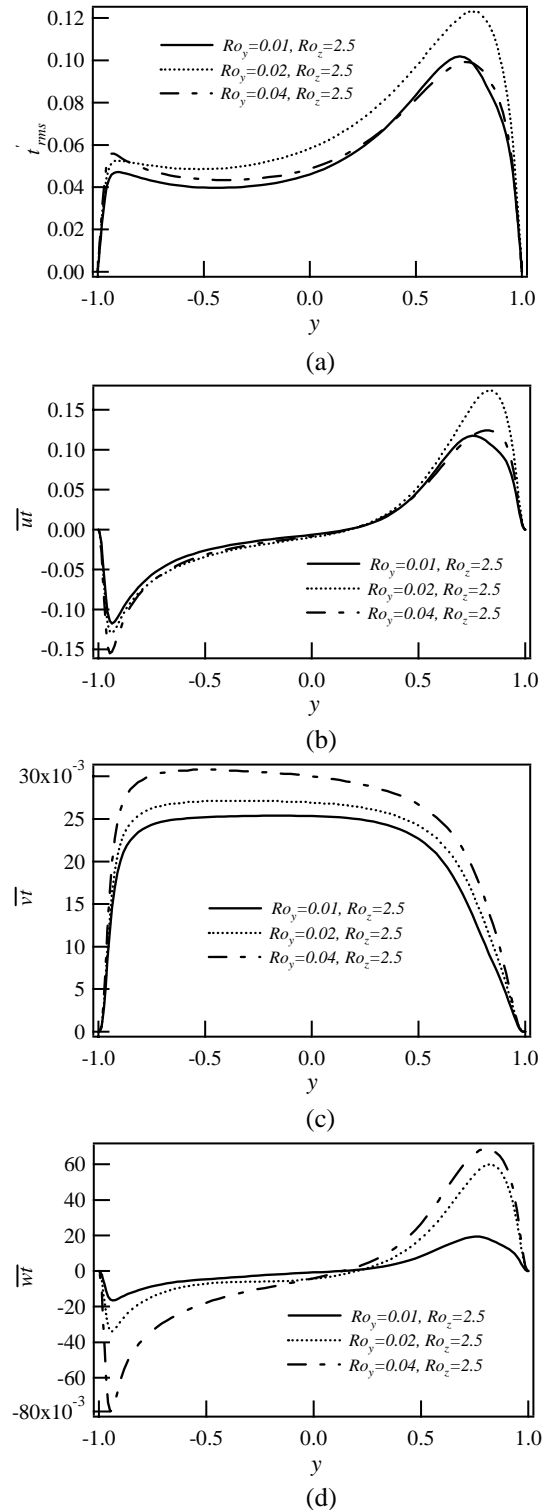

(a)

(b)

(c)

(d)

Fig. 16 Statistics in case IV (a) Rms temperature fluctuation; heat fluxes (b) $\overline{ut}$; (c) $\overline{vt}$; (d) $\overline{wt}$.

Figure 15 (a) and (b) present the streamwise and spanwise mean velocities in case IV. The bulk mean velocity in the spanwise direction is augmented by the wall-normal rotation and the profile becomes more asymmetric with respective to the center of the channel. Although W is increasingly larger, the streamwise mean velocity only change slightly and the mean temperature around the central part of the channel reduces somewhat with increasing Ro_y.

The rms temperature fluctuation and the turbulent heat fluxes are plotted in Fig. 16. The two terms t'_{rms} and $\overline{ut}$ on the suction side first increase with Ro_y, but reduce again for Ro_y larger than 0.02. The change of these two terms on the suction side is much more appreciable than that on the pressure side. The other two components of the heat fluxes, $\overline{vt}$ and $\overline{wt}$, are enhanced by the wall-normal rotation in the whole channel.

Turbulent structures in combined system rotations

Kristoffersen and Andersson [4] revealed in their DNS that the spanwise system rotation increased the number and intensity of the low- and high-speed streaks along the pressure side, while reduced them on the suction side. Elsamni [6] also found such tendency in his DNS for a spanwise rotating channel. For a streamwise rotating channel, the space between the low- and high-speed streaks is larger than the commonly observed 100 wall units in a non-rotating channel and the streaks near the upper wall and lower wall drifted towards the positive and negative z-direction, respectively. In a channel with wall-normal system rotation, the streaks along both walls tilted towards the positive z-direction. Elsamni also detected that the temperature fluctuation had some streaks between high and low temperatures correlated with the velocity fluctuation tightly.
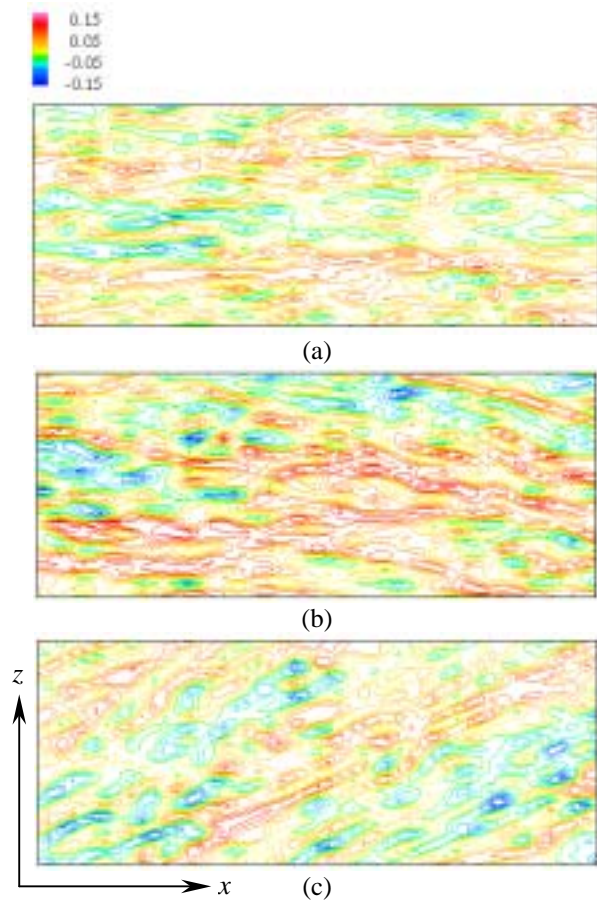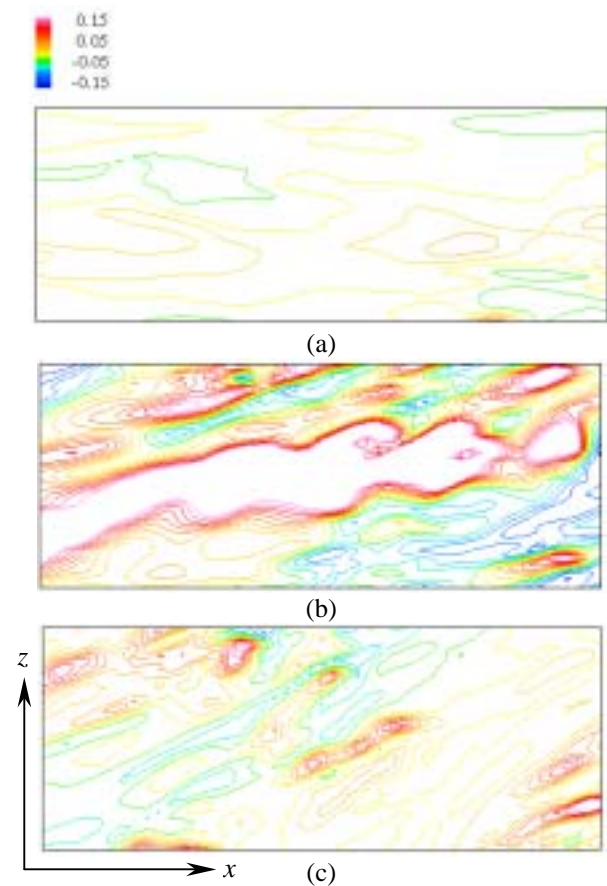

(a)

(b)

(c)

Fig. 17 Contour of temperature fluctuation in an x-z plane at $y^+ = 12.8$ near the pressure side (a) the single spanwise rotating channel $Ro_z = 5.0$; (b) the channel with combined spanwise and streamwise rotations $Ro_x = 15.0$ and $Ro_z = 5.0$; (c) the channel with combined spanwise and wall-normal rotations $Ro_y = 0.04$ and $Ro_z = 5.0$.

(a)

(b)

(c)

Fig. 18 Contour of temperature fluctuation in an x-z plane at $y^+ = 12.8$ near the suction side (a) the single spanwise rotating channel $Ro_z = 5.0$; (b) the channel with combined spanwise and streamwise rotations $Ro_x = 15.0$ and $Ro_z = 5.0$; (c) the channel with combined spanwise and wall-normal rotations $Ro_y = 0.04$ and $Ro_z = 5.0$.

Figure 17 gives the contour of the temperature fluctuation in an x-z plane at $y^+ = 12.8$ near the pressure side. In a channel with combined spanwise and streamwise rotations, the number and intensity of temperature fluctuation streaks near the pressure side are enhanced to some extent by the streamwise rotation and the streaks drift toward the negative z-direction, which coincides with the sign of the spanwise mean velocity on this side. The wall-normal rotation changes the tilting direction to the positive z-direction, but the enhancement is not so obvious as that by the streamwise rotation.

The contour of the temperature fluctuation at $y^+ = 12.8$ near the suction side is shown in Fig. 18. The spanwise rotation reduces the number of the streaks obviously on this side. In a channel with combined spanwise and streamwise rotations, however, the intensity and number of the streaks are increased evidently by the streamwise rotation and these streaks begin to point towards the positive z-direction. The wall-normal rotation makes some streaks tilt to the positive z-direction, but the intensity is much weaker than that by the streamwise rotation.

CONCLUSIONS

In the present study, the combined effect of streamwise and spanwise system rotations and that of wall-normal and spanwise system rotations are probed through a series of DNS. The findings in these two cases are concluded as follows.

In a channel with combined spanwise and streamwise system rotations, if the absolute rotation number is kept constant and just the angle between the rotating axis and positive x-direction is increased (case I), the spanwise rotation effect dominates the heat transfer. The effect of streamwise rotation can be detected from some local maxima near the suction side. The ratio of the heat flux on the wall to the total friction reaches maximum at the angle of 45°.

If the spanwise rotation number is set to 2.5 and only the streamwise rotation number is increased to 15 (case II), the heat transfer on both walls can be enhanced by the streamwise rotation, which is different from the tendency in the flow field.

In a channel with combined wall-normal and spanwise system rotations, the spanwise rotation number is increased to 15 with a constant wall-normal rotation number 0.04 (case III). In this case, the changes of most statistics with Ro_z are quite similar to those in the single spanwise rotating channel, but Nu on the both walls is comparatively larger, especially on the pressure side for Ro_z larger than 7.5.

If the spanwise rotation number is set to 2.5 and the wall-normal rotation number is increased to 0.04 (case IV), an increasingly larger spanwise mean velocity is induced, but the enhancement of Nu mainly happens along the suction side. The two components of heat fluxes $\overline{vt}$ and $\overline{wt}$ increase with Ro_y evidently.

The streaky structure of the instantaneous temperature fluctuation can be reinforced by the streamwise rotation on both walls, but the enhancement on the suction side is more noticeable than that on the pressure side. The wall-normal rotation can also increase the number of the streaky structure near the suction side, but more weakly than the streamwise rotation. The tilting direction of these streaks can be changed both by the streamwise rotation and by the wall-normal rotation.

REFERENCES

[1] Johnston, J. P., Halleen, R. M., and Lezius, D. K., "Effects of Spanwise Rotation on the Structure of Two-dimensional Fully Developed Turbulent Channel Flow", J. Fluid Mech., Vol. 56 (1972), Part 3, pp. 533-557.

[2] Kim, J., "The Effect of Rotation on Turbulence Structure", Proc. 4th Symp. Turbulent Shear Flows, Karlsruhe, 1983, pp. 6.14-6.19.

[3] Kristoffersen, R., and Andersson, H. I., "Direct Simulation of Low Reynolds-number Turbulent Flow in A Rotating Channel", J. Fluid Mech., Vol. 256 (1993), pp.163-197.

[4] Andersson, H. I., and Kristoffersen, R., "Turbulence Statistics of Rotating Channel Flow", Proc. 9th Symp. Turbulent Shear Flows, Kyoto, 1993, pp. 53-70.

[5] Oberlack, M., Cabot, W., and Rogers, M. M., "Turbulent Channel Flow with Streamwise Rotation; Lie Group Analysis, DNS and Modeling", 1st Int. Symp. Turbulence & Shear Flow Phenomena, Santa Barbara, 1999, pp. 85-90.

[6] El-Samni, O.A., "Heat and Momentum Transfer in Turbulent Rotating Channel Flow", Ph.D. diss., University of Tokyo, 2001.